*The Canadian Mineralogist*
Vol. 37, pp. 945-950 (1999)

# GORCEIXITE, A SINGULAR PRODUCT OF REPLACEMENT IN FOSSIL BONES FROM THE BAURU BASIN, BRAZIL

JOSÉ M.V. COUTINHO

*Instituto de Pesquisas Tecnológicas do Estado de São Paulo,*
*Caixa Postal 0141 – Divisão de Geologia, 01064-970 São Paulo, SP, Brazil*

DANIEL ATENCIO[§] AND ARMANDO M. COIMBRA[†]

*Instituto de Geociências, Universidade de São Paulo, Caixa Postal 11348, 05422-970 São Paulo, SP, Brazil*

LUIZ A. FERNANDES

*Departamento de Geologia, Universidade Federal do Paraná, Caixa Postal 19011, 81531-990 Curitiba, PR, Brazil*

## ABSTRACT

Gorceixite, ideally $BaAl_3(PO_4)(PO_3OH)(OH)_6$, formed by the alteration of apatite in fossil bones found in Cretaceous sandstone in the Bauru Basin, southern Brazil. The original fine structure of the bone is preserved. The presence of gorceixite was established using X-ray powder diffraction, electron-microprobe analyses and optical microscopy. No convincing evidence was found to indicate a source of Ba and Sr required for the replacement of Ca in the bone phosphate.

*Keywords*: gorceixite, fossil bone, structure, optics, chemical composition, replacement, mineralogy, Bauru Basin, Brazil.

## SOMMAIRE

Nous avons identifié la gorceixite, dont la composition idéale est $BaAl_3(PO_4)(PO_3OH)(OH)_6$, comme résultat du remplacement de l'apatite dans des os fossilisés d'un grès crétacé, bassin de Bauru, au sud du Brésil. La structure fine originelle de l'os est conservée. Nous avons utilisé la diffraction X sur poudre, des analyses à la microsonde électronique et la microscopie optique pour prouver la présence de la gorceixite. En revanche, nous ne savons rien à propos de la source du Ba et du Sr nécessaires pour effectuer le remplacement de l'apatite.

(Traduit par la Rédaction)

*Mots-clés*: gorceixite, os fossilisé, structure, propriété optiques, composition chimique, remplacement, minéralogie, bassin de Bauru, Brésil.

## INTRODUCTION

Two fossil bone fragments were found in a sandstone outcrop of the Bauru Group, approximately 2 km south of the town of Santo Inácio, Paraná State, in southern Brazil. The outcrop consists of multilevel tabular bodies (up to 1 m in thickness) of fine to very fine quartz sandstone, with minor interbedded layers of mudstone and claystone (up to 0.3 m thick), reddish to brown in color. The sandstone bodies are massive, or may show planar parallel bedding, ripple marks and climbing ripples at the top of each bed. In the internal parts of the basin, they may also present medium- to small-scale cross-bedding dipping southwest and cut-and-fill structures associated with intraclast (mudflake) breccias.

In this paper, we document this unusual occurrence of gorceixite and report a variety of physical properties and chemical data to establish its presence.

## BACKGROUND INFORMATION

The Bauru Basin is a depression developed in the south-central part of the South American Platform in the Upper Cretaceous, following the rupture of

---

[†] Deceased September 1998.

[§] *E-mail address*: datencio@usp.br

Gondwanaland and the opening of the southern Atlantic Ocean (Fernandes & Coimbra 1996a, b). Three hundred m of clastic sediments, predominantly consisting of red beds, were deposited over an erosional unconformity in the mainly basaltic Neocomian Paraná flood basalts of the Serra Geral Formation. The sequence covers an area of 370,000 km$^2$ between latitudes 18° and 24°S and longitudes 47° and 56°W, comprising parts of the Brazilian states of São Paulo, Paraná, Mato Grosso do Sul, Minas Gerais and Goiás, as well as part of northeastern Paraguay.

The Upper Cretaceous sequence is composed of two chronologically correlative groups: Caiuá and Bauru. It was deposited under a semi-arid climate, in an asymmetric endorheic basin, desertic toward its interior. Sedimentation proceeded simultaneously with the progressive uplift of the borders, defined by important positive tectonic structures, which separated it from neighboring Cretaceous basins.

## MODE OF OCCURRENCE AND GENERAL APPEARANCE

The bones were found in a sand bed exposed at a roadside cut. The host rock is a friable, clay-rich red sandstone devoid of carbonate; carbonate is, however, present as a diagenetic cement in other locations in the same sandstone formation. The depositional environment was a broad fluvial plain with shallow braided channels with sandy bars (wadis) interbedded with sand sheets. These sediments accumulated between marginal alluvial fans and desert-like deposits developed in the inland part of the Bauru Basin. Life evolved best in the northeastern part of the basin, owing to greater availability of water in the broad plains; there were plenty of streams and ephemeral alkaline lagoons. Reptiles, mostly dinosaurs, crocodiles and turtles abounded there (Coimbra *et al.* 1997). The occurrence at Santo Inácio, Paraná, constitutes the southernmost fossil record in the Brazilian Late Cretaceous and the first reported occurrence in the Bauru Group of Paraná State.

As described by Fernandes *et al.* (1994), the two whitish bones are from vertebrates, probably reptiles. They measure, respectively, 28 cm and 5 cm in length. They are both hollow with elliptical cross sections, and their internal and external structures are preserved in spite of their friable consistency. This preservation suggests that the fragments were not transported over long distances and did not undergo significant deformation after burial. The dimension and characteristics of these fragments are similar to those attributed to tetrapods, described by Fittipaldi *et al.* (1989) in the region of Pereira Barreto city (northwestern sector of São Paulo State), in the Santo Anastácio Formation (uK). When compared with other bone fossil records of the Bauru Group, the Santo Inácio bones seem to belong to reptiles. The fragmentary state of the material does not allow additional considerations about taxonomic aspects.

## OPTICAL MICROSCOPY

Three thin sections and many submillimetric fragments of bone were examined using optical microscopy. They revealed a dense, shapeless, crystalline substance of very low birefringence and occasional wavy extinction, similar to a collophane-like substance arranged in submicroscopic fibers. In a *Seismosaurus* bone, Zocco & Schwartz (1994) reported the existence of rod- and plate-shaped crystals of apatite arrayed parallel to collagen fibrils. This could also be the initial mineral composition and structure in the case of the Santo Inácio bones.

Thin sections cut transverse to the long axis of the bone (Fig. 1) show concentric lamellae, haversian canals and fibrous layers, similar to structural elements found in present-day bones. Hence, the replacement of apatite by gorceixite has not destroyed the microscopic structure of the original bone material. This may indicate pseudomorphic replacement of the original bone apatite by gorceixite.

Two types of lamella can be distinguished in sections cut parallel to the long axis of the bone (Fig. 2a). The lighter-colored and more hydrated type-A lamellae tend to replace the darker, less hydrated type-B lamellae. In Figure 2b, the neighboring lamellae A and B show apparently opposite (+) and (–) optical elongations, manifested by blue and orange yellow interference-colors. The "flash" figures obtained in both lamellae indicate that the constituent material is uniaxial (+). Its optic axis parallels the length of the lamellae with positive elongation, and criss-crosses the lamellae with negative elongation. We conclude that the bone gorceixite behaves as a palisade of fibers of positive elongation but with contrasting orientations in lamellae A and B.

Indices of refraction measured by the immersion method (Na *D* line at 20°C using Cargille liquids with an Abbe refractometer) show a slight variation among the fragments. The birefringence attained by calculation of fragment thickness and retardation remains very low and almost constant: $n_e$ in the range 1.618(2) to 1.623(2), $n_o$ in the range 1.615(2) to 1.620(2), and $n_e - n_o$ between 0.003 and 0.008. Few optical data on gorceixite have been reported after the original description by Hussak (1906) and the determination of the indices by Gaubert (1907), but they compare well with our data, with one exception; Greiffo *et al.* (1984) reported $n = 1.561(3)$, a value too low for gorceixite. They attributed such reduction to the replacement of phosphate by sulfate ions.

Several questions remain unanswered: 1) Why do the optical orientations A and B follow different (orthogonal) directions in adjacent lamellae in the bone (Fig. 2b)? 2) Why does the clear gorceixite A tend to replace gorceixite B along fissures (Fig. 2a) in spite of the fact that both types have almost the same chemical composition (see below)? 3) Why does any submillimetric fragment scraped from the bone display the negative elongation typical of apatite despite unmistakable en-

FIG. 1. Optical photomicrograph of the fossil bone in cross section as viewed under a petrographic microscope with uncrossed polarizers. Most of the original structure is intact, including the haversian canals, concentric lamellae and interstitial lamellae. The entire bone is now gorceixite. The scale bar is 1 mm.

ergy-dispersion spectra and X-ray powder-diffraction patterns indicative of gorceixite?

## X-RAY POWDER DIFFRACTION

Radoslovich & Slade (1980) and Radoslovich (1982) have refined the structure of gorceixite and concluded that the space group is monoclinic *Cm*, although strongly pseudorhombohedral $R\bar{3}m$. Blanchard (1989) obtained new X-ray powder data for gorceixite and observed a better fit of the *d* values in *Cm* than with $R\bar{3}m$ for the ICDD patterns.

Indexing of the reflections (Table 1) is given for the true monoclinic symmetry and for the pseudorhombohedral symmetry in order to compare with the structurally analogous minerals crandallite, goyazite, and florencite-(Ce). Cell parameters are summarized in Table 2.

TABLE 1. X-RAY POWDER-DIFFRACTION DATA FOR GORCEIXITE

| 1 |  | 2 |  | *hkl* | *hkl* |
|---|---|---|---|---|---|
| *d* (Å) | I (%) | *d* (Å) | I (%) | in *Cm* | in $R\bar{3}m$ |
| 5.7692 | 93 | 5.678 | 90 | $\bar{1}10, \bar{2}01+$ | 101 |
| 3.5292 | 56 | 3.490 | 56 | $\bar{3}11, 020+$ | 110, 104 |
| 3.0097 | 100 | 2.9666 | 100 | $\bar{3}12, 021+$ | 113 |
| 2.8852 | 15 | 2.8554 | 13 | $002, 220+$ | 006, 202 |
| 2.4952 | 11 | 2.4625 | 10 | $\bar{2}22, 400$ | 024 |
| 2.2925 | 39 | 2.2684 | 21 | $112, \bar{2}03+$ | 205, 107+ |
| 2.2320 | 23 | 2.2099 | 26 | $\bar{1}31, \bar{4}22+$ | 122, 116 |
| 2.0376 | 11 | 2.0162 | 10 | $\bar{1}13, 420+$ | 214, 018+ |
| 1.9197 | 29 | 1.9013 | 31 | $\bar{3}32, \bar{6}01+$ | 303, 125 |
| 1.7626 | 20 | 1.7493 | 29 | $\bar{6}22, 040+$ | 220, 208 |
| 1.6877 | 10 | 1.6685 | 5 | $\bar{5}14, 132+$ | 217, 119 |
| 1.6647 | 4 | 1.6441 | 3 | $113, 331+$ | 1 0 10, 306 |
| 1.5780 | 1 |  |  | $\bar{2}42, \bar{5}33+$ | 134, 128 |
| 1.5223 | 5 | 1.5024 | 5 | $530, \bar{7}14+$ | 315, 0 1 11 |
| 1.5058 | 18 | 1.4874 | 11 | $\bar{2}24, 402+$ | 0 2 10, 226+ |

1. Big Fish River, Rapid Creek area, Yukon Territory (Blanchard 1989).
2. Santo Inácio, Paraná, Brazil (this paper). Cu*K*α radiation.
Other reflections (*hkl*) contribute to the intensity of the peaks indicated by a +.

## CHEMICAL DATA

In Table 3, we compare the ideal composition of gorceixite with results of several chemical analyses for gorceixite found in the literature, as well as with the electron-microprobe data obtained in this study. The results obtained by Milton *et al.* (1958) on "gorceixite" from Dale County, Alabama, were not included in Table 3 because their material really is a barian goyazite.

TABLE 2. UNIT-CELL PARAMETERS FOR GORCEIXITE

|  | *a* (Å) | *b* (Å) | *c* (Å) | β(°) |
|---|---|---|---|---|
| 1 | 12.217(2) | 7.056(1) | 7.061(1) | 125.21(1) |
| 2 | 12.08(1) | 6.985(5) | 6.977(5) | 125.26(5) |

1. Big Fish River, Rapid Creek area, Yukon Territory (Blanchard 1989).
2. Santo Inácio, Paraná, Brazil (this paper).

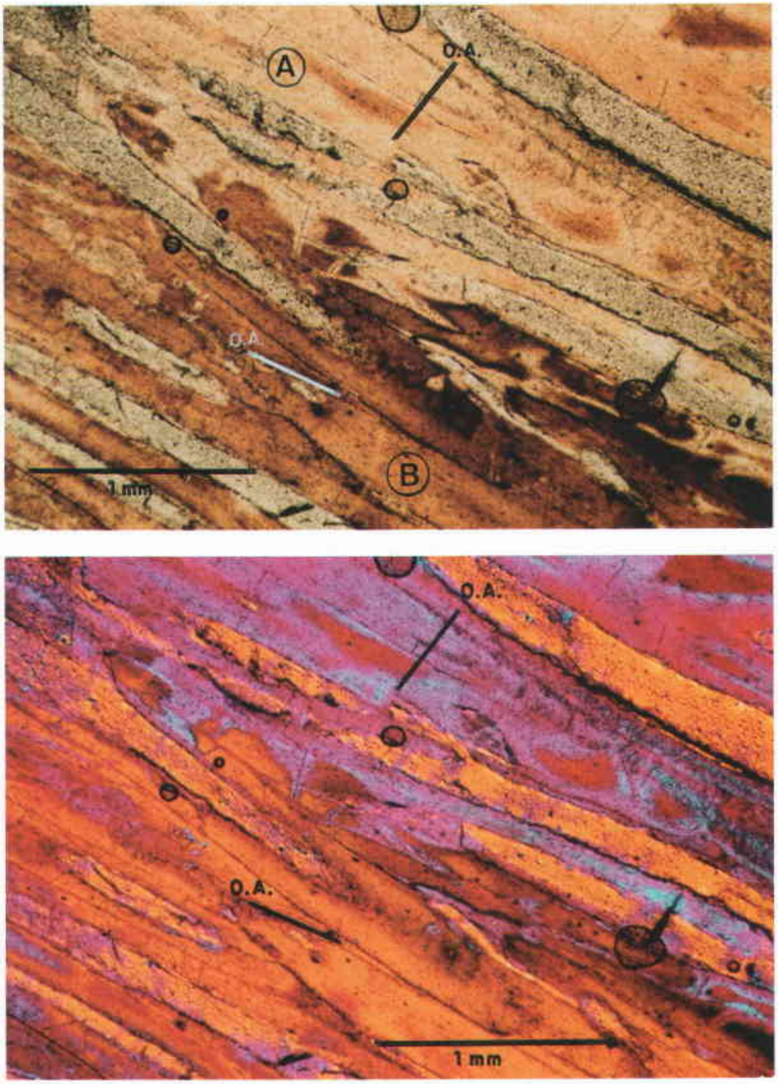

FIG. 2. Optical photomicrograph of the fossil bone depicted in Figure 1 in longitudinal section, as viewed under a petrographic microscope. Top: Uncrossed polarizers. Artificial features in this slide include round bubbles and dusty epoxy glue, filling the haversian canals. Limpid gorceixite A replaces turbid gorceixite B at the center of photo. Bottom: Between crossed polarizers, with introduction of the first-order red plate. Gorceixite lamellae A and B show blue and orange yellow interference-colors (epoxy glue is light yellow). In both photos, O.A. represents the optic axis, and the scale bar is 1 mm.

The empirical formula based on 3(Al + $Fe^{3+}$) for composition 10 is:

$(Ba_{0.55}Sr_{0.20}Ca_{0.12}Ce_{0.03}K_{0.03}Pb_{0.02})_{\Sigma 0.95}$
$(Al_{2.98}Fe^{3+}_{0.02})_{\Sigma 3.00}$ $[(PO_4)_{0.96}$
$(PO_3OH)_{0.90}(SiO_4)_{0.06}(SO_4)_{0.04}]_{\Sigma 1.96}$
$[(OH)_{5.93}(H_2O)_{0.03}]_{\Sigma 5.96}$

and for composition 11, it is:

$(Ba_{0.60}Sr_{0.21}Ca_{0.11}Ce_{0.04}Pb_{0.03}K_{0.03})_{\Sigma 1.02}$
$(Al_{2.98}Fe^{3+}_{0.02})_{\Sigma 3.00}$ $[(PO_4)_{1.00}$
$(PO_3OH)_{0.73}(SiO_4)_{0.07}(SO_4)_{0.05}]_{\Sigma 1.85}$
$[(OH)_{3.58}O_{1.31}]_{\Sigma 4.89}$.

TABLE 3. CHEMICAL DATA FOR GORCEIXITE

| | 1 | 2 | 3 | 4 | 5 | 6 | 7 | 8 | 9 | 10 | range (10) | 11 | range (11) |
|---|---|---|---|---|---|---|---|---|---|---|---|---|---|
| BaO | 30.00 | 15.42 | 18.60 | 23.52 | 16.0 | 11.88 | 19.16 | 24.00 | 26.80 | 17.84 | (16.92–19.50) | 20.09 | (19.75–20.34) |
| PbO | | | | 0.53 | | | | | | 0.73 | (0.00–1.83) | 1.52 | (0.00–3.08) |
| SrO | | | 6.35 | 1.81 | | n.d. | 7.61 | 2.95 | | 4.34 | (3.91–4.91) | 4.77 | (4.43–4.94) |
| CaO | | 3.55 | | 0.76 | n.d. | tr. | 0.61 | 0.73 | tr. | 1.45 | (1.23–1.55) | 1.29 | (1.21–1.37) |
| $Na_2O$ | | | | 0.06 | | | | | | 0.03 | (0.00–0.08) | 0.04 | (0.02–0.10) |
| $K_2O$ | | | | 0.10 | | | | | | 0.26 | (0.26–0.27) | 0.27 | (0.25–0.28) |
| $Al_2O_3$ | 29.91 | 35.00 | 31.30 | 31.25 | 35.9 | 37.96 | 30.47 | 30.02 | 26.23 | 31.83 | (30.06–32.66) | 33.14 | (32.72–33.86) |
| $Ce_2O_3$ | | 1.55$^1$ | | | n.d. | 7.00$^2$ | 0.06$^2$ | n.d. | tr. | 1.14 | (0.93–1.28) | 1.28 | (0.78–1.64) |
| $Fe_2O_3$ | | 4.10 | 0.29 | 3.76 | | 3.76 | 0.02 | 0.03 | 0.44 | 0.36 | (0.09–0.80) | 0.42 | (0.27–0.62) |
| $P_2O_5$ | 27.76 | 22.74 | 25.46 | 26.19 | 28.1 | 22.39 | 27.81 | 27.71 | 25.60 | 27.55 | (25.60–29.11) | 26.89 | (25.68–27.84) |
| $SO_3$ | | | 4.06 | | | | | | | 0.67 | (0.58–0.75) | 0.94 | (0.82–1.05) |
| $H_2O$ | 12.33 | 14.62 | 13.94 | 11.07 | 16.6 | 15.05 | n.a. | n.a. | 15.07 | 13.02 | | 8.48 | |
| $SiO_2$ | | 1.55 | | 0.95 | 1.9 | 1.25 | | | 5.15 | n.d. | | n.d. | |
| $TiO_2$ | | 0.67 | | | | | | | 0.16 | n.d. | | n.d. | |
| MgO | | | | | | 1.28 | | | | n.d. | | n.d. | |
| F | | | | | | | 4.74 | 4.19 | | n.d. | | n.d. | |
| Total | 100.00 | 99.20 | 100.00 | 100.00 | 98.5 | 96.81 | 90.51 | 89.63 | 99.45 | 100.00 | | 100.00 | |

1. Ideal chemical composition $BaAl_3(PO_4)(PO_3OH)(OH)_6$. 2. "Fava" from Rio Abaeté, Minas Gerais, Brazil (Hussak 1906). $^1$ CeO. 3. From weathered iron ore, Córrego do Feijão mine, 50 km southwest of Belo Horizonte, Minas Gerais, Brazil (Greiffo et *al.* 1984). 4. Formerly "ferrazite", Diamantina, Minas Gerais, Brazil (Atencio & Clark 1996). 5. Concretions in weathered carbonatite, Mrima Hill, Kenya (Coetzee & Edwards 1959). 6. Pebble in Triassic gravel, Somabula, Southern Rhodesia (MacGregor 1941). $^2$ $CeO_2$. 7 and 8. Topaz greisen, Silvermine area, Missouri (Taylor *et al.* 1984). $^2$ $CeO_2$. 9. Product of weathering, Chadobets Uplift, Siberia (Serdyuchenko & Chayka 1967). With some opal. 10. Fossil bone, Santo Inácio, Paraná, Brazil. Region A in Figure 2 (this paper). Average result of four analyses; $H_2O$ by difference. 11. Fossil bone, Santo Inácio, Paraná, Brazil. Region B in Figure 2 (this paper). Average result of five analyses; $H_2O$ by difference. The proportion of $H_2O$ reported in columns 3 and 4 also is calculated by difference. Standards used for electron-microprobe analyses of domains A and B (anal. 10 and 11): $BaF_2$ (Ba), galena (Pb), celestine (Sr), wollastonite (Ca), plagioclase (Na), microcline (K), corundum (Al), $CeAl_2$ (Ce), hematite (Fe), InP (P), and chalcopyrite (S). n.a.: not determined, n.d.: not detected, tr.: traces.

## ORIGIN

No convincing evidence was found to indicate a source of Ba and Sr necessary to produce gorceixite by the replacement of an apatite-group phase.

## ACKNOWLEDGEMENTS

We acknowledge financial support by CNPq (Conselho Nacional de Desenvolvimento Científico e Tecnológico), grants 30.2025/76–6 and 30.6413/88–4, and FAPESP (Fundação de Amparo à Pesquisa do Estado de São Paulo), grants 93/4524–9 and 96/0669–0. The manuscript has benefitted from perceptive reviews of I. McReath, H.C.W. Skinner, J.M. Hughes, R.F. Martin and J. Rakovan.

## REFERENCES

ATENCIO, D. & CLARK, A.M. (1996): Ferrazite is identical to gorceixite. *Mineral. Mag.* **60**, 841-842.

BLANCHARD, F.N. (1989): New X-ray powder data for gorceixite $BaAl_3(PO_4)_2(OH)_5 \cdot H_2O$, an evaluation of d-spacings and intensities, pseudosymmetry and its influence on the figure of merit. *Powder Diffraction* **4**(4), 227.

COETZEE, G.L. & EDWARDS, C.B. (1959): The Mrima Hill carbonatite, Coast Province, Kenya. *Trans. Proc. Geol. Soc. S. Afr.* **62**, 373-395.

COIMBRA, A.M., COUTINHO, J.M.V., FERNANDES, L.A. & BRANDT NETO, M. (1997): Vertebrate taphonomy in Bauru Basin (Upper Cretaceous, Brazil). *Anais da Academia Brasileira de Ciências* **69**(2), 270-271.

FERNANDES, L.A. & COIMBRA, A.M. (1996a): A Bacia Bauru (Cretáceo Superior, Brasil). *Anais da Academia Brasileira de Ciências* **68**(2), 195-205.

________ & ________ (1996b): Estratigrafía y ambientes deposicionales de la Cuenca Bauru (Cretácico Superior, Brasil). *Acta Geol. Hispànica* **30**(4), 11-30.

________, ________ & HACHIRO, J. (1994): Contexto paleoambiental de ocorrência de ossos de vertebrado no Grupo Bauru (Ks), Estado do Paraná, Brasil. *Boletim Paranaense de Geociências* **42**, 113-119.

FITTIPALDI, F.C., FERNANDES, L. A., SIMÕES, M.G. & COIMBRA, A.M. (1989): Primeira ocorrência de tetrápodes na Formação Santo Anastácio (Cretáceo da bacia do Paraná). *In* Congresso Brasileiro de Zoologia, 89-90.

GAUBERT, M.P. (1907): Sur les indices de réfraction de quelques minéraux. *Bull. Soc. Fr. Minéral.* **30**, 104-109.

GREIFFO, W., HERRMANN, K., MÜLLER, G. & STRAUSS, K.W. (1984): Sr-gorceixite, a weathering product in rich iron ores from the Córrego do Feijão mine, Minas Gerais, Brazil. *Contrib. Mineral. Petrol.* **87**, 418-419.

HUSSAK, E. (1906): Über die sogenannten "Phosphat-Favas" der diamantführenden Sande Brasiliens. *Tschermaks Mineral. Petrogr. Mitt.* **25**, 335-344.

MACGREGOR, A.M. (1941): Gorceixite from Southern Rhodesia. *Bull. Imp. Inst. London* **37**, 399- 401.

MILTON, C., AXELROD, J.M., CARRON, M.K., STEARNS, F. & MACNEIL, F.S. (1958): Gorceixite from Dale County, Alabama. *Am. Mineral.* **43**, 688-694.

RADOSLOVICH, E.W. (1982): Refinement of gorceixite structure in Cm. *Neues Jahrb. Mineral., Monatsh.*, 446-464.

________ & SLADE, P.G. (1980): Pseudo-trigonal symmetry and structure of gorceixite. *Neues Jahrb. Mineral., Monatsh.*, 157-170.

SERDYUCHENKO, D.P. & CHAYKA, V.M. (1967): Geochemical history of phosphorus and barium during the genesis of carbonatite-like rocks and old residuum of the Chadobets Uplift. *Dokl. Acad. Sci. USSR, Earth Sci. Sect.* **177**, 224-226.

TAYLOR, M., SMITH, R.W. & AHLER, B.A. (1984): Gorceixite in topaz greisen assemblages, Silvermine area, Missouri. *Am. Mineral.* **69**, 984-986.

ZOCCO, T.G. & SCHWARTZ, H.L. (1994): Microstructural analysis of bone of the sauropod dinosaur *Seismosaurus* by transmission electron microscopy. *Paleontology* **37**, 493-503.

*Received March 27, 1997, revised manuscript accepted July 24, 1999.*